

# LAYOUT OF THE DIAGNOSTIC SECTION FOR THE EUROPEAN XFEL

Ch. Gerth, M. Röhrs, H. Schlarb\*

Deutsches Elektronen-Synchrotron DESY, D-22603 Hamburg, Germany

## Abstract

Fourth generation synchrotron light sources, such as the European Free Electron Laser (XFEL) project, are based on an exponential gain of the radiation amplification in a single pass through a long undulator magnet. To initiate the FEL process and to reach saturation, precise monitoring and control of the electron beam parameters is mandatory. Most challenging are the longitudinal compression processes in magnetic chicanes of the high brightness electron bunch emitted from an RF photo-injector. To measure and control the beam properties after compression, careful consideration has to be given to the design of a diagnostic section and the choice of beam monitors. In this paper, the proposed layout of one of the XFEL diagnostic beamlines is discussed.

## INTRODUCTION

The European Free Electron Laser (XFEL), which will generate laser-like, femtosecond radiation down to the Ångstrom wavelength region, is being designed as a multi-user facility [1]. The electron beam will be distributed into several undulator beamlines for the generation of FEL radiation based on the principle of self-amplified spontaneous emission (SASE). As the FEL amplification process is based on exponential gain, the FEL radiation is extremely sensitive to the electron beam parameters. The electron beam tailoring for high peak currents and ultrashort bunch lengths is achieved in several steps mitigating diluting effects such as coherent synchrotron radiation during the magnetic bunch compression or space charge effects at low beam energies. Sophisticated beam diagnostics is indispensable for the commissioning of the FELs as well as on-line beam monitoring during machine operation especially in open loop systems like linear accelerators. The principle accelerator layout of the European XFEL facility is shown in Fig. 1. Two dedicated diagnostic sections (denoted as DS1 and DS2) for the full characterization of the beam properties are located downstream of the bunch compressors at beam energies of 0.5 GeV and 2.0 GeV, respectively. The main beam and linac parameters are summarized in Table 1. In this paper, we focus on layout issues of the diagnostic sections 1.

## DIAGNOSTIC SECTIONS

The major objectives of the diagnostic sections, which need to be taken into consideration for the layout and design of these beamlines, are the full characterization of the

Table 1: Main beam and linac parameters

| Parameter           | Variable     | Units         | Value |
|---------------------|--------------|---------------|-------|
| Charge              | Q            | nC            | 1.0   |
| Norm. emittance     | $\epsilon_n$ | $\mu\text{m}$ | 1.0   |
| Beam energy BC1     | $E_{BC1}$    | GeV           | 0.5   |
| Bunch length BC1    | $\sigma_z$   | $\mu\text{m}$ | 100   |
| Energy spread       | $\sigma_E/E$ | %             | 1.8   |
| Momentum compaction | $R_{56}$     | mm            | 100   |
| Beam energy BC2     | $E_{BC2}$    | GeV           | 2.0   |
| Bunch length BC2    | $\sigma_z$   | $\mu\text{m}$ | 20    |
| Energy spread       | $\sigma_E/E$ | %             | 0.4   |
| Momentum compaction | $R_{56}$     | mm            | 20    |

projected beam parameters (emittance, longitudinal bunch profile, energy spread) with high accuracy, the possibility of monitoring single bunches within bunch trains, the measurement of slice parameters and the reconstruction of the phase space distribution by tomography. The diagnostic devices should also offer the possibility to act as feedback systems for the stabilization of beam parameters against slow drifts. The overall lattice design of the diagnostic section should allow for a well-defined matching into the subsequent linac sections.

The diagnostic section 1 (DS1) comprises two transverse deflecting cavities (TCAVs), one for each plane, which will enable measurements of slice emittances and longitudinal bunch profiles. This is accomplished by imaging systems based on optical transition radiation (OTR) which are located in a FODO lattice for multi-screen emittance measurements. Fast kickers and off-axis screens are being considered for the on-line monitoring of individual bunches. The deflected off-axis bunches are dumped in an absorber downstream of DS1. Bunch compression monitors (BCM), which are based on an intensity measurement of the coherent synchrotron radiation emitted by the last dipole of the bunch compressor, will be used as fast regulators for the low-level radio-frequency for phase stabilization. Electro-optical devices are foreseen for the permanent and parasitic measurement of timing jitter and longitudinal bunch profiles. For commissioning, a spectrometer magnet followed by a high dispersion section will be used for precise energy spread measurements.

Figure 2 shows the matched  $\beta$ -functions in DS1 from the exit of first bunch compressor to the entrance of the following linac section obtained with the code MAD8. In order to increase the resolution of the TCAVs, relatively large  $\beta$ -functions ( $\beta \simeq 15$  m) are required at the location of the TCAVs and small  $\beta$ -functions at the location of the

\*Holger.Schlarb@desy.de

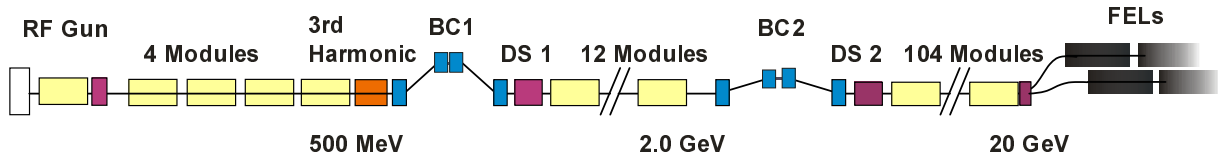


Figure 1: Accelerator layout of the European XFEL Project (BC: bunch compressor; DS: diagnostic section).

OTR screens in the subsequent FODO lattice. Small  $\beta$ -functions in the FODO lattice, which in this example has a  $22.5^\circ$  phase advance per cell and 7 cells, are also desirable with regards to a short overall length and small space charge effects (see below). A relatively large  $\beta$ -function is then required for the matching into the accelerating module due to the widely spaced focusing elements in the linac.

Table 2: FODO lattice parameters.

| $\Psi_{cell}$ | OTRs. | No. cells | $L_{tot}^*$ [m] | $L_{tot}^{**}$ [m] |
|---------------|-------|-----------|-----------------|--------------------|
| $22.5^\circ$  | 8     | 7         | 13.1            | 26.7               |
| $30.0^\circ$  | 6     | 5         | 12.4            | 25.3               |
| $45.0^\circ$  | 4     | 3         | 11.0            | 22.4               |
| $60.0^\circ$  | 3     | 2         | 9.4             | 19.3               |
| $67.5^\circ$  | 8     | 5         | 26.0            | 53.2               |

\*  $E = 500$  MeV;  $70 \mu\text{m}$  beam size;  $\epsilon_n = 1 \mu\text{m}$

\*\*  $E = 2$  GeV;  $50 \mu\text{m}$  beam size;  $\epsilon_n = 1 \mu\text{m}$

## EMITTANCE MEASUREMENTS

The aim is to measure the projected and slice emittances with an accuracy in the percentage range in a non-disruptive pulse stealing mode. A promising solution appears to be fast kickers that can be used to deflect individual bunches onto multiple off-axis screens. If the transfer matrices from one location in the lattice to the screens are precisely known, measurements of the beam widths on at least three screens allow the determination of the beam Twiss parameters at this location as well as the projected emittances (usually referred to as the standard multi-monitor method).

The best options for lattices for emittance measurements are FODO lattices with phase advances per cell listed in Table 2, and OTR-screens located in the centers of the drift sections. The Table compares the No. of measurements (OTR stations), No. of cells and the total lengths of the lattices.

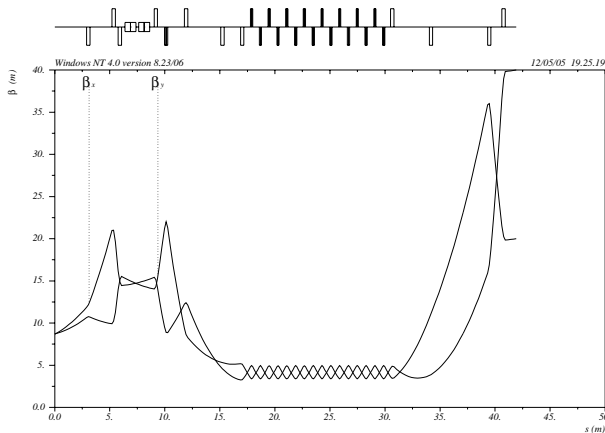


Figure 2: Evolution of the  $\beta$ -functions in the diagnostic section 1.

## Error Analysis

Errors of the calculated Twiss parameters and the geometric emittance are due to measurement errors or jitter of the beam sizes or due to deviations of the actual beam transfer from the assumed linear transfer. In the latter case the caused beam size deviations at the screens are crucial. In this section, we discuss the results for some error sources considering as examples the differences between the  $22.5^\circ$  and  $45^\circ$  FODO lattice. All simulations were performed with the beam parameters specified in Table 2 for DS1.

**Systematical Errors** A main source for systematic errors are deviations of the actual beam energy from the measured one. This effects the beam transfer as well as the calculated normalized emittance through the relativistic parameter  $\gamma_{rel}$ . The resulting emittance error depends strongly on the Twiss parameters of the beam at the entrance of the FODO lattice, and the errors nearly vanish if the beam Twiss parameters are matched to the periodic solution for the actual beam energy [2]. In the case of a mismatch, the  $22.5^\circ$  and  $45^\circ$  FODO lattices show different resulting errors depending on the specific matching condition and neither of them show a significant advantage. In order to keep the emittance error below 1% for moderately mismatched beams ( $M \approx 2$ , see [3]), the energy error needs to be less than 1%. The energy can be monitored on-line in the upstream bunch compressor.

To investigate random quadrupole gradient errors Monte Carlo simulations have been performed. The  $22.5^\circ$  lattice shows a slightly larger sensitivity to gradient errors. To keep the emittance error below 1% with a probability of 98% in the case of a perfectly matched beam, the gradient errors have to be below 0.3% and 0.4% for the  $22.5^\circ$  and  $45^\circ$  FODO lattice, respectively.

Random transverse misalignments of quadrupoles in a

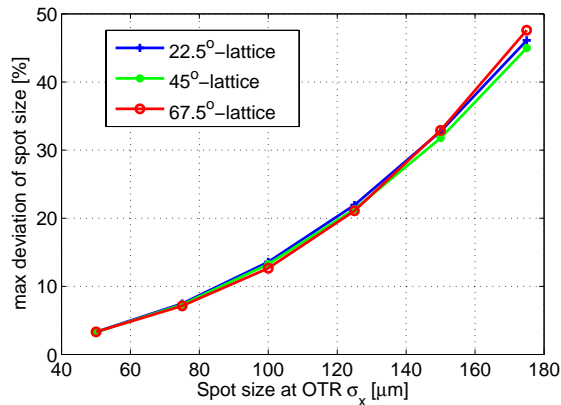


Figure 3: Maximum deviation from the nominal beam size due to space charge for different nominal beam sizes and FODO lattices calculated with the linear approximation.

FODO lattice lead to deflections of the beam centroid and an accumulation of dispersion. The dispersion may lead to an increase of the beam size and scales linearly with the quadrupole misalignment error. Hence, larger beam sizes would be desirable regarding quadrupole misalignment errors which is in contrast to space charge effects. As an example, for a 22.5° FODO lattice with a nominal beam size of 70  $\mu\text{m}$  and a given energy spread 1.8% the rms quadrupole alignment error needs to be smaller than 100  $\mu\text{m}$  in order to keep deviations of the beam size at the OTR stations below 2%.

Space charge forces and chromaticity also effect the beam widths at the diagnostic stations. From a linear approximation [4] it was found that the maximal beam size deviation due to space charge scales proportionally to the square of the beam sizes and is almost independent of the phase advance per cell as can be seen in Fig. 3. Simulations with the particle tracking code ASTRA [5] yield a maximum deviation of about 2% for a beam size of 50  $\mu\text{m}$ . Beam size deviations due to chromaticity have been found to be negligible for an energy spread of 1.8%.

In case of uncorrelated calibration errors of OTR monitors the resulting emittance errors scale proportionally to the square root of the number of monitors used, the relative emittance error being equal to the relative beam size measurement error in the case of 4 monitors. Systematic calibration errors and systematic errors in the image analysis result in a relative emittance error of twice the relative beam size error, independent of the used lattice.

*Statistical Errors* If the measured beam sizes are subject to statistical errors, the resulting emittance error is found to be minimal when the beam size measurements are performed at equal phase advance intervals covering 180°. The dominating sources for statistical errors are (i) jitter of the betatron functions and (ii) statistical errors in the image analysis. For both types we have assumed that the beam size error scales proportionally to its width. Under this as-

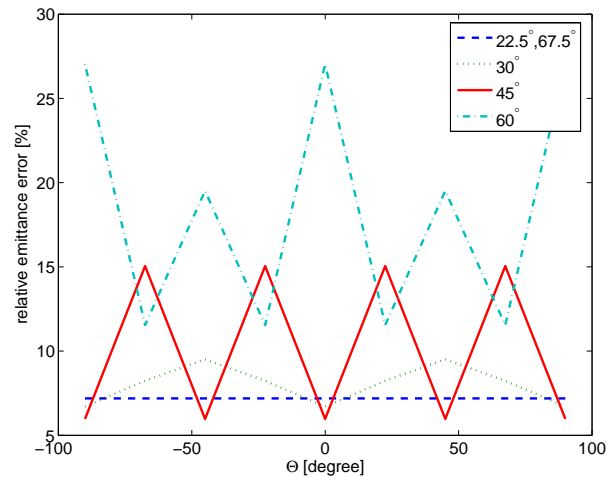


Figure 4: Resulting emittance errors as a function of  $\Theta$  for  $M = 4$ , a beam size error of 10% and total of 16 beam size measurements for all lattices.

sumption, the resulting emittance error is smallest for equal beam sizes at all diagnostic stations, which is the case if the beam is matched. The resulting emittance error is proportional to the square root of the total number of beam size measurements and independent of the considered lattices. For an initial mismatch described by the mismatch parameter  $M$  and mismatch phase  $\Theta$  [3], the beam sizes may vary from screen to screen. Figure 4 shows the emittance errors as a function of  $\Theta$  for a fixed  $M = 4$  for various lattices. It can be seen that a lattice with a smaller phase advance per cell is less sensitive to the mismatch phase.

## SUMMARY

Layout considerations for the diagnostic sections at the European XFEL project have been presented. Emphasis has been put on layout issues for a FODO lattice for multi-screen emittance measurements. The error analysis for the 22.5° and 45° lattices has not revealed a clear preferences for either of these lattices. However, the 22.5° lattice seems to be more promising for slice emittance measurements and tomography methods which are currently under study.

## REFERENCES

- [1] A. Schwarz, "The European X-Ray Free Electron Laser Project at DESY", FEL2004, Trieste, August 2004.
- [2] P. Castro, "Monte Carlo simulations of the emittance measurements at TTF2", DESY Technical Note, September 2003, DESY.
- [3] M. Sands, "A Beta mismatch parameter", SLAC-AP-085, 1985.
- [4] L. Teng, "PRIMER ON BEAM DYNAMICS IN SYNCHROTRONS", FERMILAB-TM-1475, 1987, Fermilab.
- [5] K. Flöttmann, "ASTRA User Manual", September 18, 2000. <http://www.desy.de/~mpyflo>.